CERN-ACC-NOTE-2023-0023

18-12-2023

Giulia.Bellodi@cern.ch

Conceptual design study for a dedicated low-energy diagnostics line at Linac3

G Bellodi, D Bodart, J-M Cravero, J Extebarria Erdoiza, D Kuchler, E Mahner, F Roncarolo, R Scrivens*
CERN, Geneva, Switzerland
C A Valerio Lizarraga
Universidad Autonoma de Sinaloa, Mexico

Keywords: ions, diagnostics, Linac3, low-energy

Abstract

A low-energy diagnostics upgrade of Linac3 has been studied in the last couple of years to allow a more precise characterization of the beam properties at extraction from the source, currently impeded by a complete lack of measuring devices in the first ~6 m of the accelerator layout. Due to space tightness constraints, the solution explored consists of a dedicated beam diagnostics line, branching off the main lattice through a 90^{o} spectrometer magnet. Through a choice of pulse-to-pulse functionality, this solution would also allow permanent logging in operation and the implementation of feedback loops that could help achieve better source performance stability. This note details the design and beam dynamics performance of this line, and it provides a preliminary assessment on feasibility and costing.

Contents

1. Introduction

A Linac3 low-energy diagnostics upgrade was studied in the last few years as a solution to overcome the current lack of measuring devices in the first part of the machine layout, and thus allow for a more precise ion beam characterization at extraction from the source. The study was conducted within the framework of the OXY4LHC project [1] at CERN, and progressed thanks to the contribution of an external collaborator from the University of Sinaloa (Mexico), co-author of this report.

The design that was explored is that of a dedicated diagnostics line branching off the operational Linac3 machine lattice through a 90 degrees spectrometer bend, to be fitted in the existing layout a few meters downstream of the source. With added pulse-to-pulse functionality, this solution would also allow the possibility of permanent logging of beam parameters in parallel to normal operation (as half of the beam pulses of the 10Hz pulsed source could be diverted to the diagnostics line without compromising the present performance of the downstream complex). This would be particularly significant/important in the study and setting up of beam extraction for non-standard new types of ions that might be requested by physics experiments at CERN in the near future (Mg, Kr, etc – see Table 2 for more details).

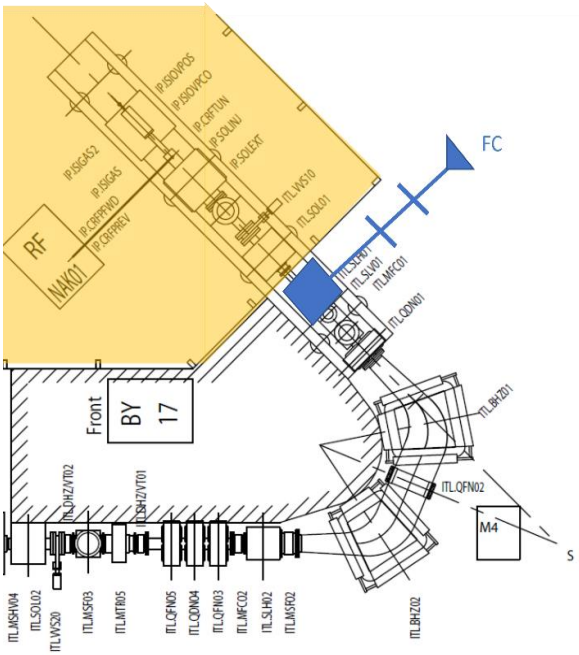

Fig. 1: Sketch of the low-energy section of Linac3 showing the proposed location of the new diagnostics line (in blue). The source cage area is marked in yellow.

2. Linac3 source and LEBT

Heavy ion beams are produced at Linac3 with the GTS-LHC 14.5 GHz ECR ion source. The source is operated in afterglow mode with 10 Hz repetition rate and 50 ms RF heating pulse length. At the end of the 50 ms the microwaves are stopped, and the ions are released more quickly, leading to a higher peak intensity from the source for a few milliseconds (afterglow). The intensity of the beam during the afterglow is continuously changing. A 200 μs long slice is then selected from the afterglow peak and accelerated at up to 5 Hz repetition rate through the Linac3 RF cavities. The time structure of the beam

is shown in Fig. 2, where a 2D surface plot shows the beam intensity as a function of q/m (charge-over-mass ratio) and time.

Different ion species can be produced at Linac3, by changing the material delivered to the source. Elements available in gaseous form (or as a compound gas) can be injected through a flow control valve. Metals with sufficiently high vapour pressure can be evaporated using the micro-ovens. For each ion species, the source requires the settings of some ten parameters to be optimized. There is no direct measurement of the total beam current from the source, nor a precise knowledge of space charge compensation effects in this zone.

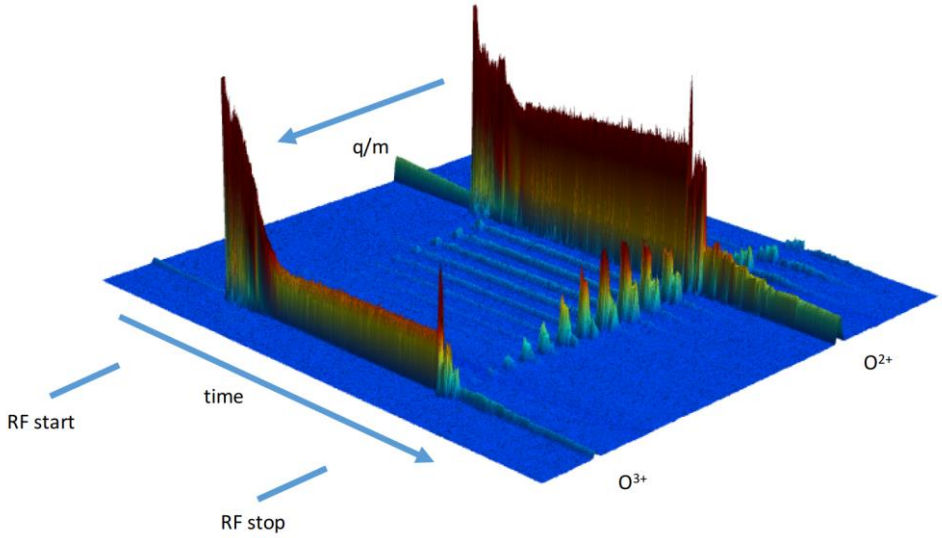

Fig. 2: Time structure and composition of the beam at source extraction in afterglow mode

In the first section of the Low Energy Beam Transport (LEBT) all the ion charge states extracted from the source are present. Due to the difference in momentum for each ion type, the first focusing elements (a solenoid and a quadrupole) act on each ion type differently.

Two bending magnets in the LEBT function as a spectrometer with the magnetic fields set to transport the desired ion type through the correct angle. Other ions are either lost on the walls of the vacuum chamber of the spectrometer, or on dedicated slits (ITL.SLH02) at the spectrometer exit, which are set at a defined aperture to select the requested ion species to be transported downstream.

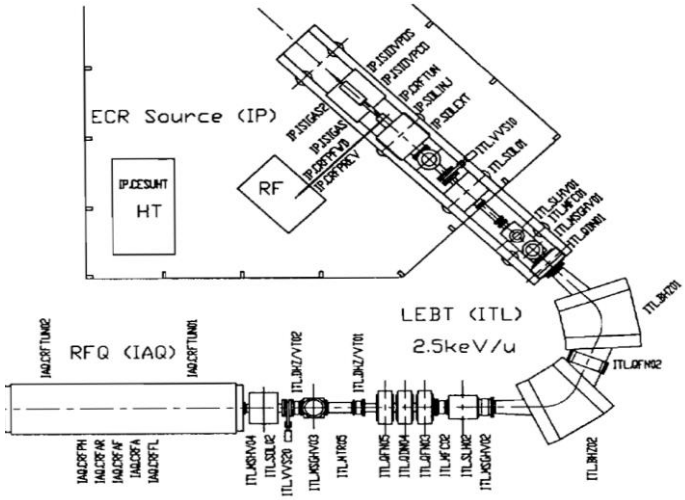

Fig. 3: Layout of the low-energy part of Linac3.

There are no diagnostics devices available in this initial part of the accelerator, where the beam is formed. First characterization in the transverse planes is only possible downstream of the slit, via beam profile measurements on a SEMgrid device. A Beam Current transformer and Faraday Cup are also installed in the vicinity for beam intensity measurements and characterization of the spectrum of ion species extracted from the source via Charge State Distribution (CSD) scans. These devices being mostly of a destructive type, measurements can only be performed either during the beam commissioning setup at the yearly restart of operations, or during dedicated time slots for beam studies, when beam delivery for physics is temporarily stopped. All magnet power supplies in this section are also DC, and do not offer a pulse-to-pulse functionality that could be exploited to make use of the additional pulses from the source that are not accelerated downstream.

3. Low-energy diagnostics line layout

A study was therefore launched in 2020 within the framework of the OXY4LHC project [1] to design a dedicated low-energy diagnostics line that could be used parasitically for beam investigations without affecting the nominal operational performance of the downstream complex for which Linac3 acts as the main injector.

A 1.2 m long free space was identified between the ITL.SOL01 solenoid and ITL.QDN01 quadrupole, that could accommodate a 90^{o} pulsed dipole diverting the beam into a new diagnostics line (see Fig.4). At this location a 2.8 m long clearance is available before interfering with equipment racks along the back wall.

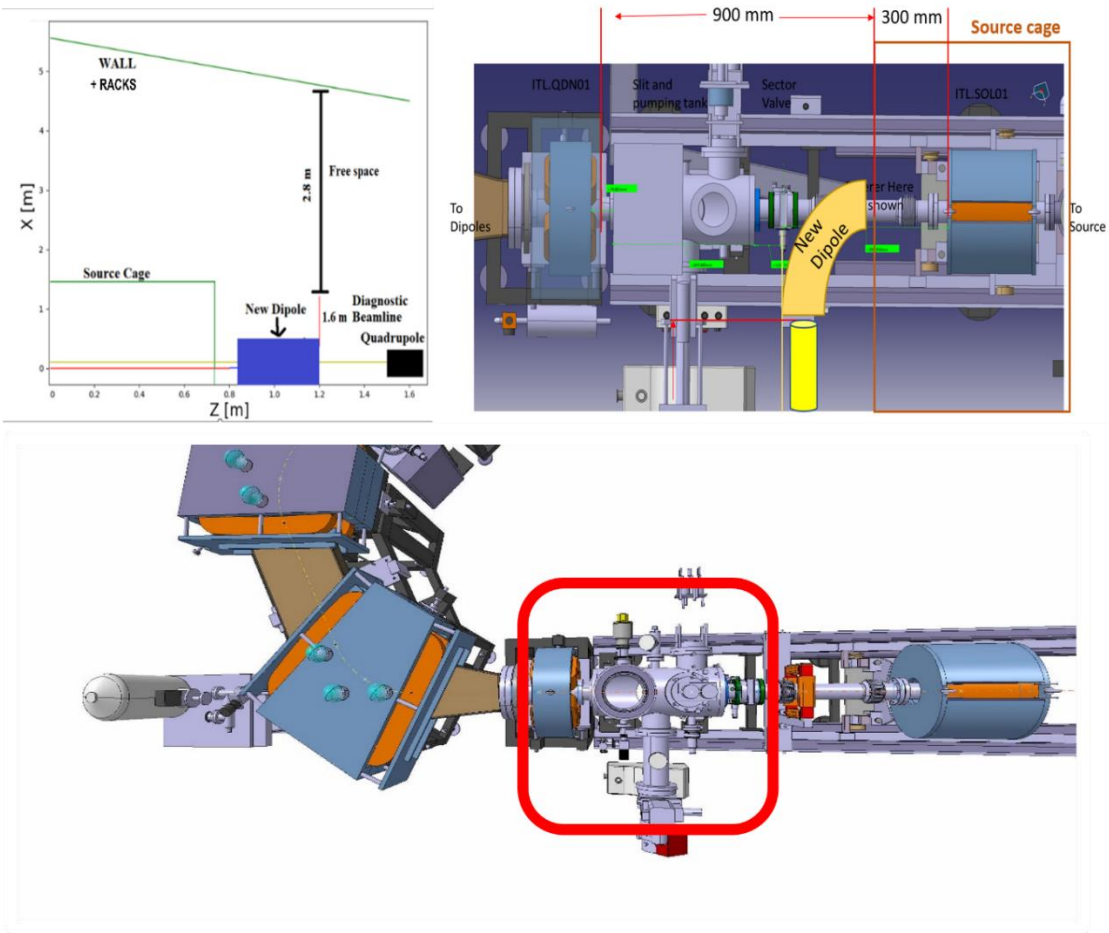

Fig. 4: Proposed location for installing a bending magnet to divert the Linac3 beam in a dedicated low-energy diagnostics line.

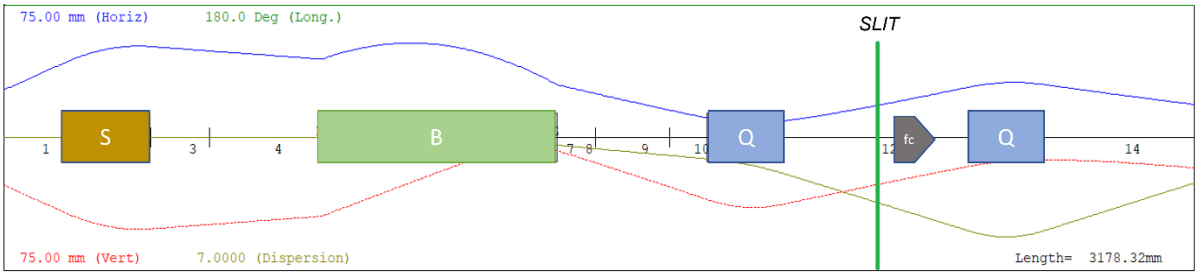

Fig. 5: Simulation of the beam diagnostics line with Trace3d. Maximum axis values for dispersion and beam envelopes are 7 m and 75 mm respectively in the above plot.

The diagnostics line would start at the position of this bending magnet and continue over a length of a couple of meters along a straight line where additional magnets and instrumentation devices will be installed. The beam dynamics simulation of the line using Trace3d [2] is shown in Fig.5, together with the total beam envelopes in both transverse planes. Two quadrupoles are placed downstream of the bending magnet to add flexibility in beam focusing. A slit and Faraday Cup (FC) are needed for charge state distribution scans. Additional diagnostics instruments for transverse beam characterization (profiles and emittance) are planned to be installed downstream of the second quadrupole, but their exact location has not been defined yet in the present study**.**

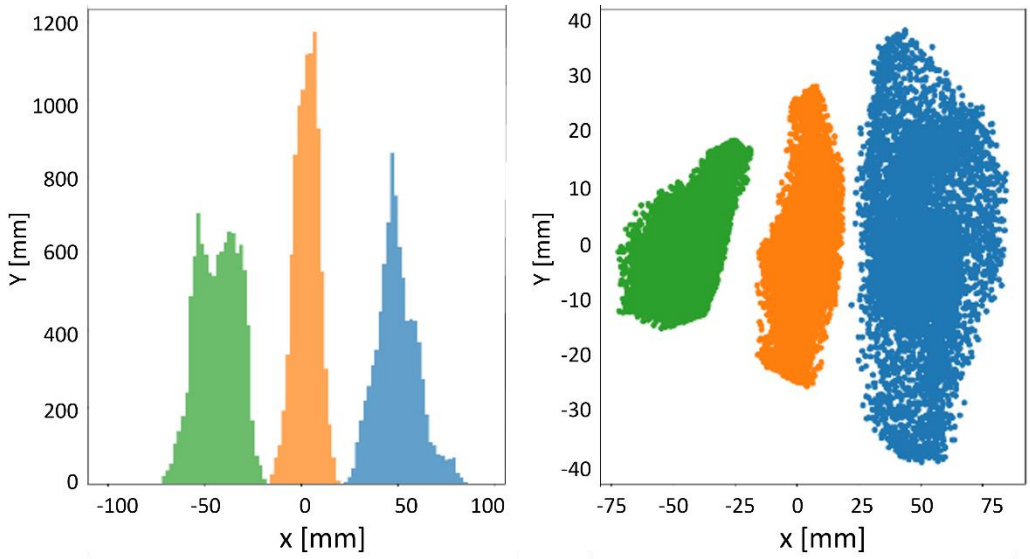

Fig. 6: Separation between Pb29+ and adjacent charge states (28+, 30+) at the FC position.

A key element in the definition of this layout is the line dispersion, which determines the separation between adjacent charge states at the measurement plane. The design of the diagnostics line and positioning of the various elements was optimised to maximise the dispersion and thus achieve a sufficient resolution in charge state distribution (CSD) measurements at the Faraday Cup. For a dipole bending radius of ρ =400 mm and θ =90° angle the drift length $\boldsymbol{l}$ must be > 0.8 m. The inclusion of the defocusing quadrupole in the line improves the dispersion up to 2.6 m at 0.8 m after the dipole. A minimization routine has been implemented using TRAVEL [3] with Python to scan parameters like the solenoid strength and dipole faces rotations and find the optimal dispersion and final beam size configurations. The TRACE 3D code has been used to confirm the results. All calculations and studies were carried out for the nominal $^{208}Pb^{29+}$ central ion beam at an energy of 2.5 keV/u. The input beam distribution has been obtained by modelling the source extraction with the IBSimu code [4]. It was found that for the present settings of Linac3 for Pb^{29+} operation there are beam losses before the existing

spectrometer, so in order to achieve a lossless transmission the aperture of the solenoid needs to be increased from its current 10 cm to 13 cm. The envelope presented here refers to the zero-space charge case, this case being also the one with the lower dispersion D= 2.6 m. The transverse beam dynamics simulation and beam matching at the end of the line was optimised to keep the 3 RMS horizontal beam size smaller than the separation between adjacent charge states peaks, to as be able to clearly distinguish the different contributions to the beam current on the monitor. Figure 5 shows the beam envelope evolution in Trace 3D: the horizontal and vertical envelopes are contained within the suggested apertures in the line. Figure 6 shows the separation for Pb^{29+} and adjacent charge states at the FC position.

3.1 Magnets specifications

A bending radius of 0.4 m has been chosen for the dipole magnet, the same as in the already installed ITL spectrometer magnets. For this value of ρ the field necessary to bend the Pb^{29+} beam is 0.132 T. The edge angles of the magnet have been calculated through a minimization routine to increase the line dispersion and decrease the beam size at the slit/Faraday Cup location. Table 1 summarises the dipole parameters. The dipole needs to be pulsed at 10 Hz to deliver the beam to the diagnostic line. It will be desirable for the power supplies to have a 0.1% stability. The maximum field variation in the good field region of the dipole should not exceed 1%.

Table 1: Bending magnet parameters.

Dipole parameter	**Value**
Bending radius [m]	0.4
Effective length [m]	0.628
Nominal central B field (Pb^{29+}) [T]	0.132
Bending power $\int B.dl$ [Tm]	0.083
Bending angle [deg]	90
Vertical aperture [m]	0.1
Rotation in Face 1 β_1 [deg]	39
Rotation in Face 2 β_2 [deg]	39
Horizontal aperture [m]	0.2

New ion species requests have been advanced for post-LS3 operation by both fixed target and LHC experiments, which are now under discussion and feasibility assessment [5]. Sufficient flexibility needs to be built in the design of the diagnostics line to satisfy these future operational requests. The dipole magnet should be able to transport to the diagnostics line other ion beams besides $^{208}Pb^{29+}$, still extracted from the source at an energy of 2.5 keV/u for the main charge state. Table 2 lists the ion species presently under discussion. Calcium and Magnesium are the elements with the highest A/q ratios, requiring the highest magnetic field value of 0.23/0.25 T respectively to bend the +2/+1 charge state. Therefore 0.25 T has been taken as the maximum B field value in the conceptual study of the dipole magnetic model by TE-MSC.

The upstream ITL.SOL01 solenoid magnet will also need to be adapted to the transport of different ion species and upgraded to pulsed operation instead of DC. Table 3 lists the necessary current values for focusing the ion types presently under discussion, just rescaling with beam rigidity from the present operational settings. The solenoid needs to be pulsed, or allow its field to be changed in 10-20 ms, and requires a beam pipe aperture of 130 mm.

Table 2: Dipole field requirements for the various ion beam candidates currently under discussion for post-LS3 operation at Linac3.

Element	Main charge state	q/A	Extraction voltage [kV]	B Field Max [T]	B Field main charge state [T]
Oxygen [+1,8]	4+	0.25	10.0	0.144	0.072
Argon [+5,15]	11+	0.275	9.6	0.100	0.065
Calcium [+2,18]	5+	0.125	20.0	0.228	0.144
Krypton [+5,20]	11+	0.131	19.1	0.118	0.137
Xenon [+15,30]	22+	0.171	14.7	0.128	0.105
Lead [+20,40]	29+	0.139	18.8	0.159	0.129
Helium [1,2]	1+	0.25	10.0	0.072	0.072
Lithium [1,3]	1+	0.143	17.5	0.126	0.126
Boron [1,5]	2+	0.182	13.75	0.140	0.099
Magnesium [1,8]	3+	0.125	20.0	0.249	0.144

Table 3: Solenoid magnet operational current requirements for the list of ion beam candidates under discussion for post-LS3 operation.

Element	Main charge state	q/A	Extraction voltage [kV]	Max current [A]	Current for main charge state [A]
Oxygen [+1,8]	4+	0.25	10.0	278.8	69.7
Argon [+5,15]	11+	0.275	9.6	139.4	63.4
Calcium [+2,18]	5+	0.125	20.0	348.6	139.4
Krypton [+5,20]	11+	0.131	19.1	292.8	133.1
Xenon [+15,30]	22+	0.171	14.7	149.9	102.2
Lead [+22,40]	29+	0.139	18.8	181.3	125
Helium [1,2]	1+	0.25	10.0	69.7	69.7
Lithium [1,3]	1+	0.143	17.5	122	122
Boron [1,5]	2+	0.182	13.75	191.7	95.9
Magnesium [1,8]	3+	0.125	20.0	418.3	139.4

Finally, a pair of quadrupole magnets will be used after the dipole to transport the beam to the end of the line without incurring beam losses and to improve flexibility in the beam specifications at selected diagnostics locations. For design simplicity the quadrupoles have been assumed to share the same properties as all other ITL quadrupoles in the main beam line. Table 4 shows the quadrupole

parameters, where the maximum gradient is set at 2.7 T/m (for nominal operation with Pb^{29+} beams it is close to 1 T/m). The quadrupoles must be able to pulse with the same timescale as the bending magnet or be DC.

Table 4: Quadrupole magnets parameters.

Quadrupoles parameter	Value
Pole length [mm]	150
Effective length [mm]	204
Aperture (diameter) [mm]	120
Max gradient [T/m]	2.7

3.2 Transverse beam dynamics

The design of the diagnostics line has been validated through beam dynamics simulations using Travel and Trace3D codes and an input beam distribution obtained by modelling the source extraction of ^{208}Pb with the IBSimu code [6], see Fig.7.

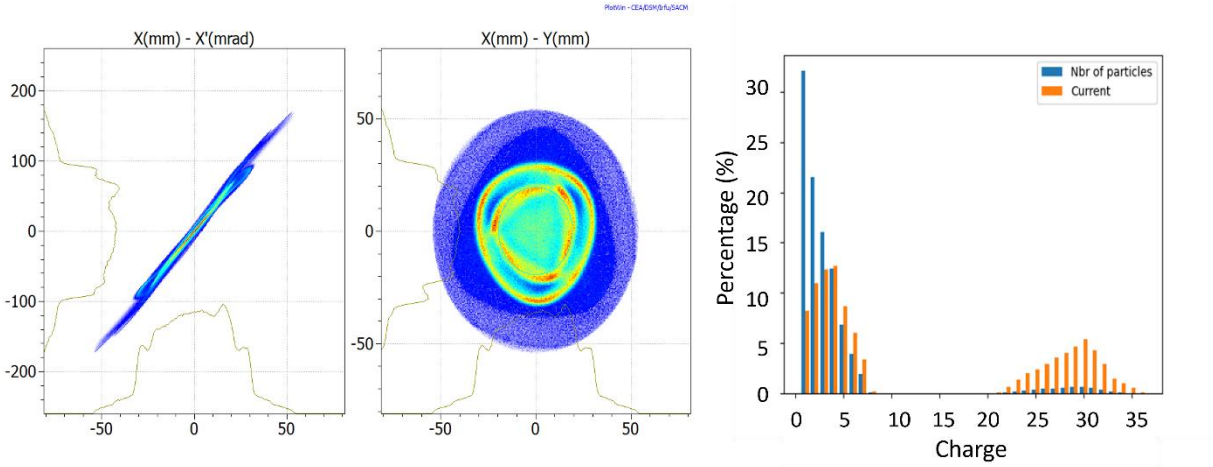

Fig. 7: Pb^{29+} input beam distribution at source extraction as obtained from IBSimu simulations. From left to right: x-x', x-y phase space distributions and a histogram of the different charge state contributions (Lead and Oxygen).

Since the first priority for the diagnostics line would be the ability to carry out charge state distribution measurements parasitically to beam operation, the beam dynamics design was validated through an assessment of the resolution achievable in such measurements (namely the degree of separation between adjacent charge states). Space charge was found to have quite an influence on the quality of the final results. Since the total beam current at source extraction is not precisely known, nor are the exact mechanisms of space charge compensation along the line, different space charge assumptions have been taken into account in the studies and the results have been compared. The simulations that were carried out try to reproduce exactly the measurement steps of the scan, with an optimization of the line settings for the transport of each different charge state one by one (varying the ion momentum, solenoid strength and dipole bending field). This exercise was repeated for 1 mA and 4.5 mA ^{208}Pb input beam currents. Good transport efficiency to the Faraday Cup and a neat separation between adjacent states were the goals to be obtained for each charge state case. Fig.8 shows the simulation results for transporting different ^{208}Pb charge states, from q=22+ to q=35+ in the case of a

1mA total input beam current. For each of them the top plot shows the beam current distribution (current histogram) that would be recorded at the Faraday Cup position, while the bottom plot shows the particles distribution in the physical x-y phase space (as scatter plot), also at the FC location. Even in cases where some contamination from adjacent charge states is present, these are quite neatly separated at the FC, with the only exception of $^{208}Pb^{26+}$ and $^{16}O^{2+}$, that even in practice cannot be distinguished due to their identical charge/mass ratio. Similar results are obtained in the assumption of a higher 4.5 mA input beam current, requiring just ~5% stronger solenoid fields for beam focusing.

The quality of the results obtained has therefore been taken as final validation of the beam dynamics design of the diagnostics line.

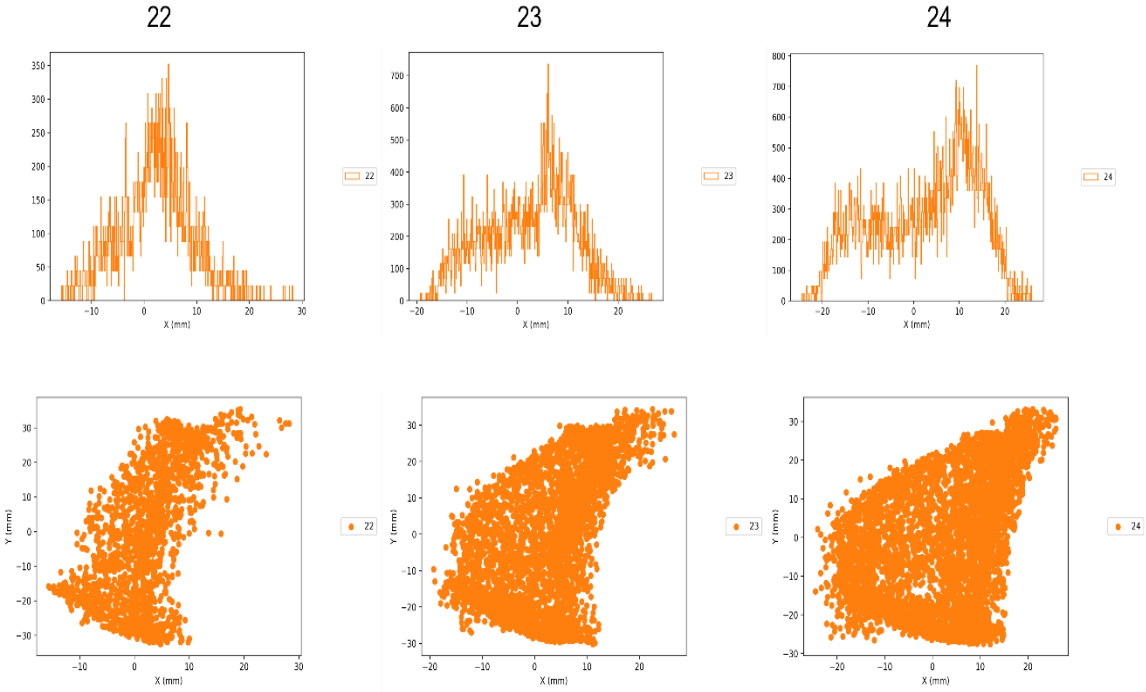

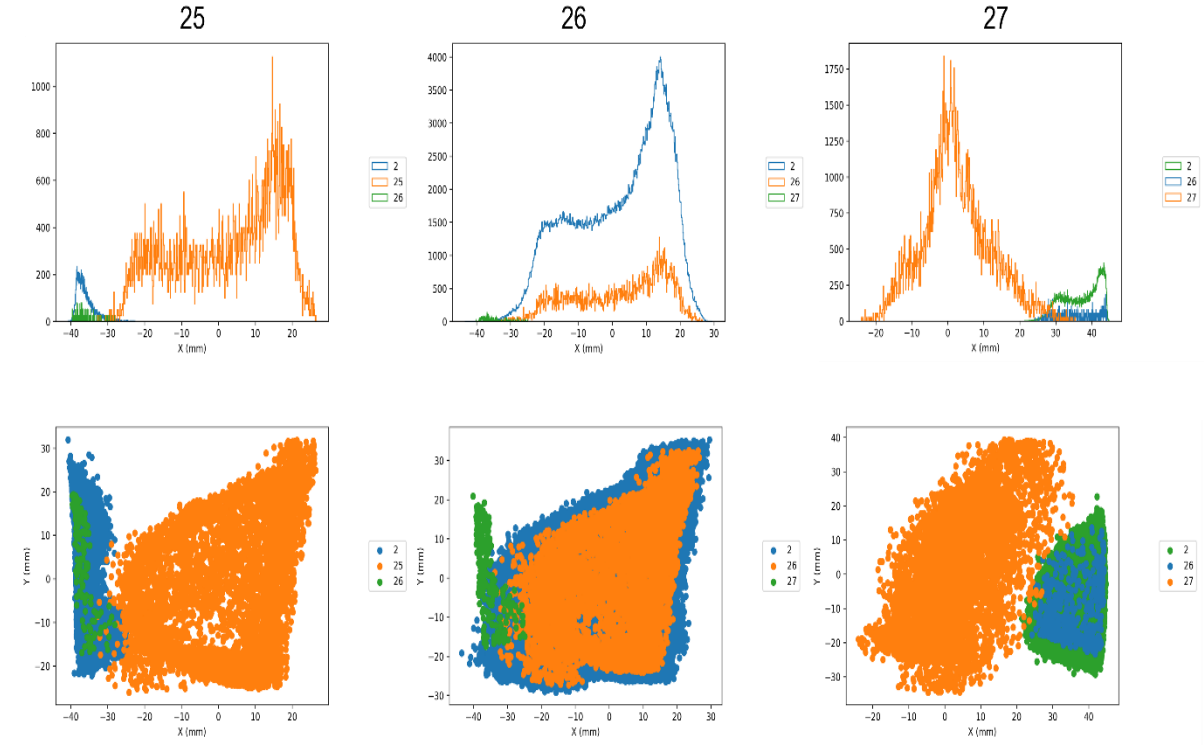
25
26
27
X (mm)
Y (mm)
2
25
26
27

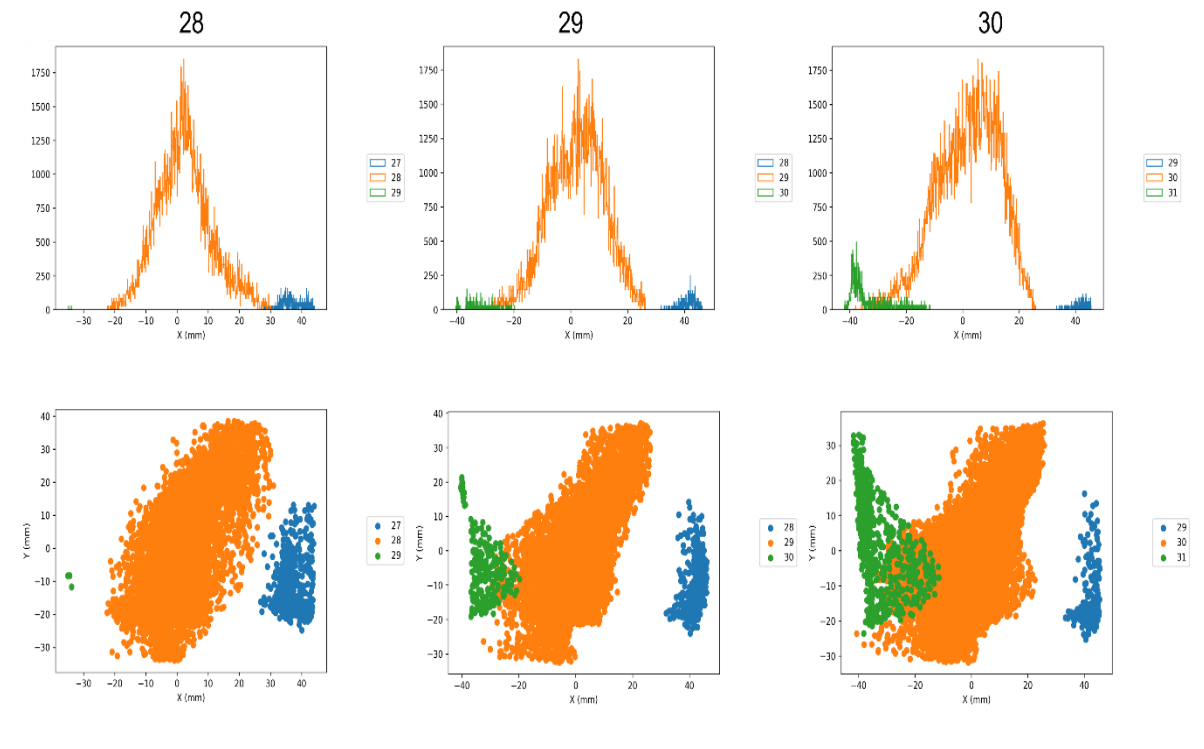
28
29
30
X (mm)
Y (mm)
27
28
29
30
31

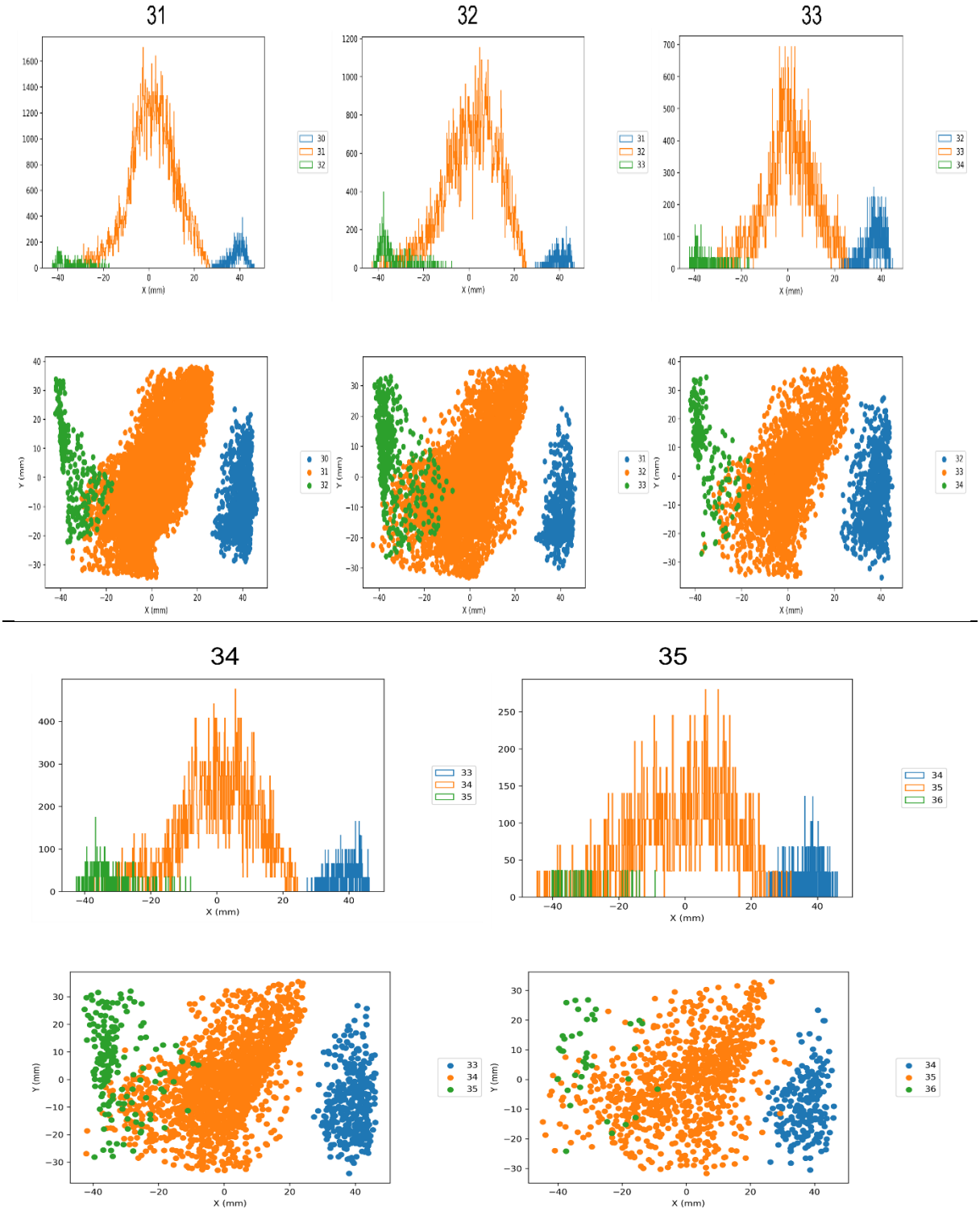

Fig. 8: Simulated CSD scan measurement results for a 1mA input Pb^{29+} beam current (beamline optics settings are modified to optimize the transport of individual charge states in the spectrum). For each charge state (number at the top) two plots are shown: the top one shows a histogram of the current profile at the FC, while the bottom one (scatter plot) shows the beam distribution in the x-y space at the same location. These plots are used to predict the contamination of different charge states (green and blue) other than the main wanted one (in orange) in the measurements.

4 Diagnostics

The new Linac3 diagnostics line should allow a full beam characterization shortly after source extraction. In addition to parasitic charge state distribution measurements (agreed to be the main priority), the goal would be to characterize the beam in the transverse plane via 2D beam profile measurements (not just one plane projections) and transverse emittance measurements. As lower priority, longitudinal plane characterization should be added to the list, via energy and energy spread measurements.

The beam pulse from the source is ~50 ms long, with only the last few ms long after-glow constituting the 'useful' beam being transported and accelerated downstream. Diagnostics devices need to be capable to properly characterize these few milliseconds of beam, ideally with a resolution of 5 μs.

After a series of meetings with SY/BI colleagues, a preliminary list of instrumentation requests has been defined, together with initial costing estimates and assessment for feasibility and implementation. The discussed list of instrumentation includes:

- a Beam Current Transformer (BCT) and a Faraday Cup (FC) for beam current measurements,
- a BTV station (or equivalent device, as a segmented FC for example) for 2D beam imaging,
- an emittance meter (of the slit/SEMgrid or Allison Scanner type) for transverse emittance measurements.

The BTV station and slit/SEMgrid type of emittance meter using stepping motors represent existing technology and design, and they have therefore been assumed as baseline choice for initial discussions and for putting together a preliminary budget and feasibility estimate [7].

The choice of BCT hardware is challenging due to the wide range of beam intensities to cover (~0.5 to hundreds of μA for different ion species) and the long integration times (milliseconds). One solution could be to install a fast-BCT for higher intensity beams and one electrostatic ring (pick-up) for lower intensity beams (to be cross-calibrated with the former). Digital acquisition could be either through a TRIC card (now getting obsolete) or PCI digitizers. The total cost for the two units is estimated at ~110 kCHF, covering hardware, electronics and acquisition (without cabling).

A BTV station would be ideally composed of a screen installed at 45 deg inclination, inserted either through a push-pull actuator driven by a stepping motor or through a standard pneumatic IN-OUT mechanism. The material choice for the screen would have to be the result of dedicated R&D, specially addressing thermal aspects and beam-induced damage. It would be interesting to conceive a system allowing multiple screens insertion, thus working at the same time as a bench for testing different screen types. Screen size/acceptance and vacuum quality requirements still need to be assessed. A preliminary cost estimate is in the order of 40 kCHF, covering the costs of the screen hardware and insertion device, the vacuum tank, camera and electronics, but without including the cost of cables nor vacuum sectorization provisions, if deemed to be necessary.

A slit+SEMgrid emittance meter, similar to what was built for the Linac4 test stands is estimated to cost around 100 kCHF, with breakdown details available in [7].

Finally the Faraday Cup is estimated to cost around 20 kCHF, bringing the total instrumentation budget for the proposed list of devices to ~270 kCHF (only for the devices, and not control, acquisition, cabling and integration).

On top of theese cost estimate uncertainties, no personnel resources are presently available in SY/BI to focus on this project. Should the upgrade plan be approved for installation during LS3, one extra GRAD or QUEST would be needed for 1-1.5 years.

5 Magnet design and power converters

The bending magnet is a new design sector magnet bending the beam by 90 degrees in the horizontal plane. The magnet specifications are listed in Table 1. The magnet will be located near the exit of the solenoid ITL.SOL01, the best location being shown in the sketches of Fig. 9 and 10 (side and top view respectively). The maximum B field initially assumed in the studies is of ~0.3 T (needed for transporting Ca^{1+}), though a lower value of 0.25 T has also been taken into account in the following to ease the magnet design (though this will require relaxing the CSD scan range for Calcium to a minimum charge state of 2+). A preliminary magnetic modelling of the magnet (shown in Fig.10) has resulted in the construction specifications listed in Table 5.

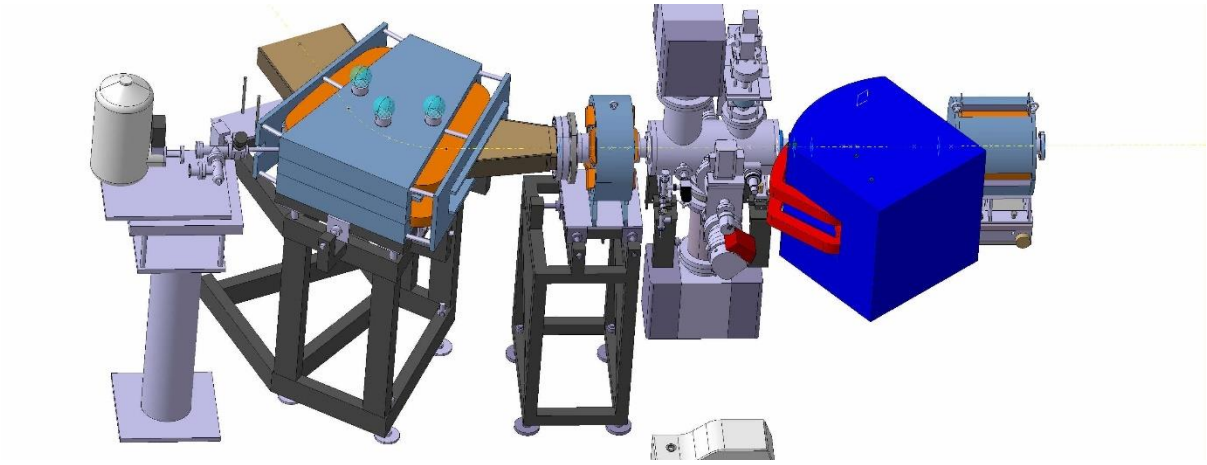

Fig. 9: 3D side view of the magnet position

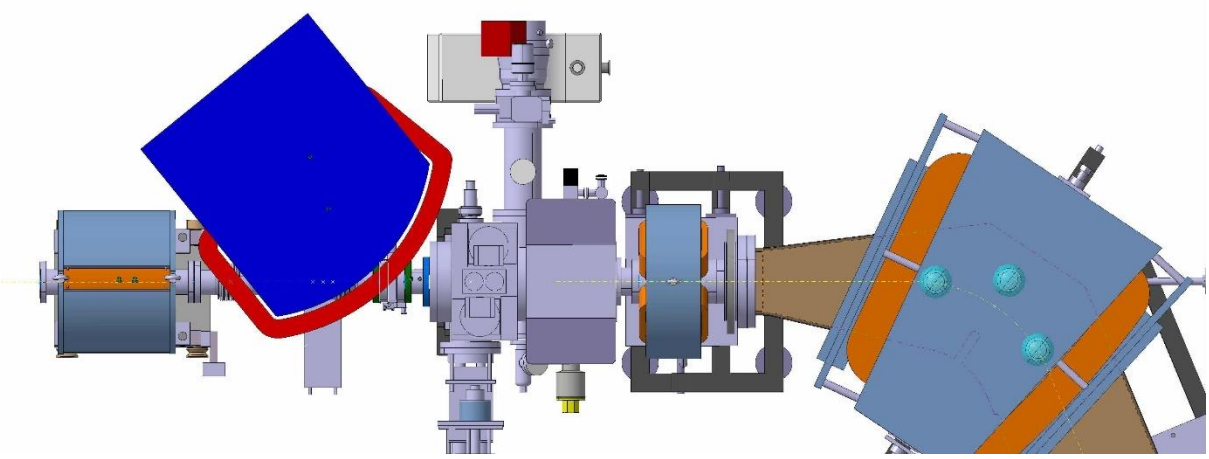

Fig. 10: 3D top view of the magnet position.

The estimated costs of production of the bending magnet with a set of spare coils is approximately 80 kCHF, including magnetic measurements and supporting structure. Design office costs are estimated at 25 kCHF.The lead time for the procurement, reception, installation and commissioning is about 1.5 years.

The specifications in Table 5 have been used to study available options for the bending magnet powering. The bending magnet needs to be pulsed with 100 ms repetition rate and with short rise and

fall times. The powering solution is to use a MegaDiscaP converter that is usually employed to power septum and bending magnets in the PS complex transfer lines (Booster, AD, LEIR, etc…), where fast pulses with short rise and fall times and high precision flat-top are needed. The MegaDiscaP converter delivers a current with a trapezoidal waveform shape. Initial specifications were to have the entire pulse contained if possible in less than 1ms, for easier operational conditions of the BCT hardware downstream. This however would require major changes in the existing converter designs, thus increasing the risks and the global costs and manpower needed.

It has therefore been decided to relax the rise and fall times requirements and investigate the best possible options with an existing MegaDiscaP converter design. Following an optimisation of the magnet parameters to be compatible with the MegaDiscaP power converter specifications, the optimal design is that of a magnet coil with 18 turns. The MegaDiscaP power converter specifications are given in Table 6.

Table 5: Bending magnet specifications after magnetic modelling.

Bending magnet specifications	**Value**
Number of turns	18
Coils resistance	15 mΩ
Magnet inductance	0.9 mH
Conductor size	8 x 8 mm
Operating current at B=0.25T	1105 A
Operating current at B=0.3T	1326 A

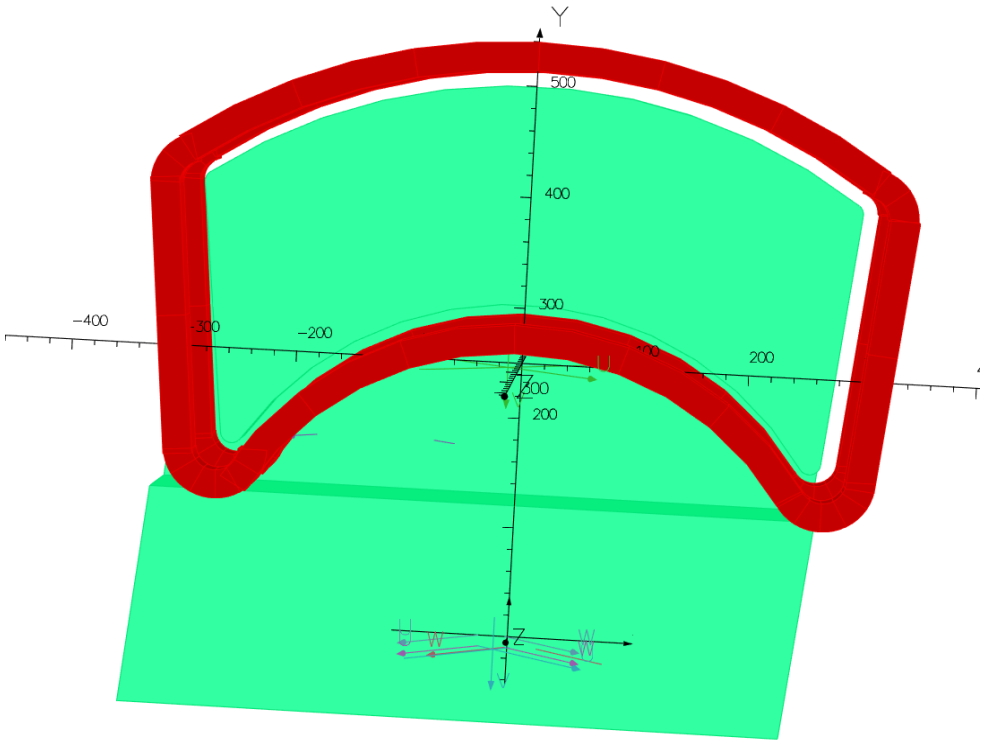

Fig. 11: View of the dipole magnet 3D magnetic model.

Table 6: MegaDiscaP power converter parameters.

MegaDiscaP converter parameters	**Units**	**Value**
Maximum operating current	[A]	1400
Minimum operating current	[A]	300
Current precision	[A]	± 2.5
Maximum output voltage	[V]	2000
Magnet current rise time at 0.25T	[ms]	0.7
Magnet current rise time at 0.30T	[ms]	0.85
Maximum flat-top duration	[ms]	2
Repetition time	[ms]	100
Operation mode		p.p.m.
Remote control		FGC3 (Class 62)
Input voltage (3 phases with neutral)	[V_{RMS}]	400
Maximum input current (per phase)	[A_{RMS}]	40
Cooling		Forced air
Dimensions (width × depth × height)	[mm]	1150 × 1000 × 2225
Weight	[kg]	750

The MegaDiscaP converter uses three capacitor chargers to load large capacitor banks (C1, C2 and C3) used as energy storage. With 100 ms repetition rate, the capacitor chargers of the standard MegaDiscaP converter have to be replaced by more powerful units. Such capacitors charger units are available directly from the supplier and they can be installed in the MegaDiscaP racks with minor modifications. The shape of the magnet is given in Figure 11 and the power converter trapezoidal current with its reference set to 1105 A (operation at 0.25 T) is shown in Fig.12.

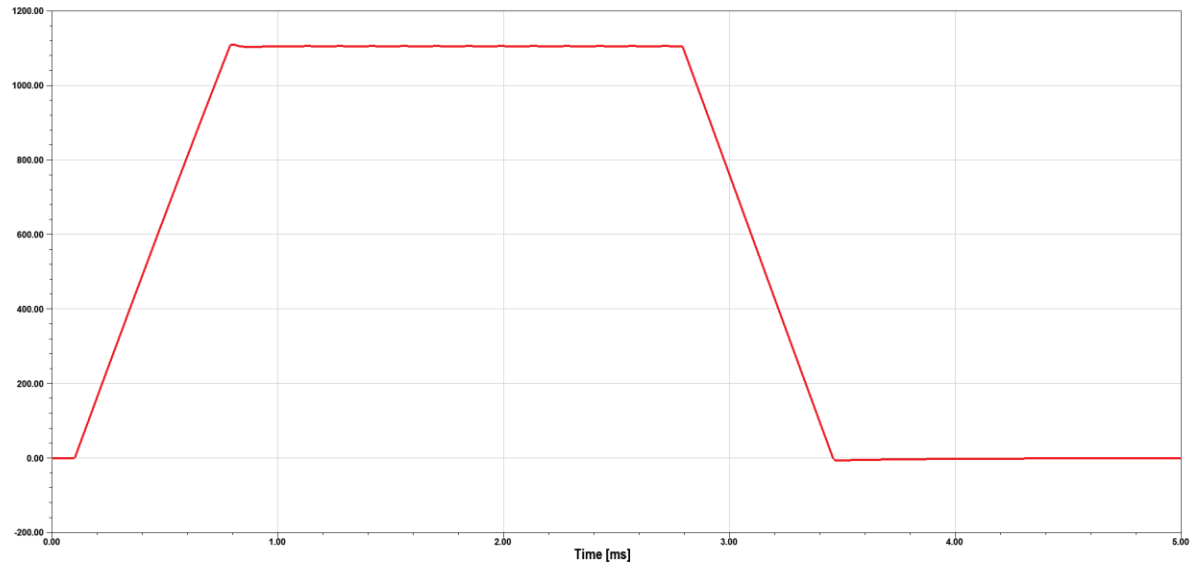

Fig. 12: Magnet current with I_{ref} = 1105 A (0.25 T) and flat-top duration set to 2 ms.

The MegaDiscaP power converter for this application can be installed in building 363 where three converters of the same type will be installed for the powering of PI.SMH26 and ER.SMH40 with a spare. With this option, no additional spare converter is required. For a single converter, the total budget cost is 100 kCHF and the converter production can be scheduled for an installation during LS3 if the decision is taken in 2024. The cost of cabling (AC, DC, ethernet, interlocks, etc..) and installation in building 363 (metallic support, false floors, etc…) are not included in this first estimate.

The existing solenoid magnet ITL.SOL01 is a magnet type PXMLNAAIWP with a solid yoke. It is made of a series of 21 coils of 32 turns each with independent cooling circuit. An outer thick shell made of magnetic steel surrounds the coils and participates to the magnetic flux by focusing the return flux perpendicularly to the beam trajectory on both ends.

Table 7: Present ITL.SOL01 solenoid magnet parameters.

Present solenoid basic parameters	**Value**
Free mechanical aperture diameter [mm]	110
Nominal field [T]	0.42
Nominal magnetic length [m]	0.3
Nominal current [A]	220
Number of turns	21x32=672
Nominal resistance at 20 °C [mΩ]	435
Nominal dissipated power [kW]	21.1
Pressure drop [bar]	1
Cooling flow [l/min]	15.9
Water temperature increase [°C]	20
Overall length [mm]	320
Overall width [mm]	392
Overall height [mm]	500
Total mass (approx..) [kg]	180

Table 8: New solenoid magnet requirements.

New solenoid magnet parameters	**Value**
Inductance [mH]	16
Resistance at 20°C [mΩ]	450
Maximum operating current [A]	400
Repetition time [ms]	100
Operation mode	p.p.m.

For the operation of the new measurement line, the magnet current must be increased to 400 A peak. Also, the magnet and associated power converters have to be operated in pulse-to-pulse operation mode with 100ms pulse spacing. In this context, the magnet yoke will be replaced by a laminated version. The outer shell shall be made of laminated steel plates. Furthermore, magnetic modelling shows

saturation on the iron core when the magnet is operated at an electrical current of 400 A. The current magnet parameters are listed in Table 7 and the new solenoid requirements in Table 8.

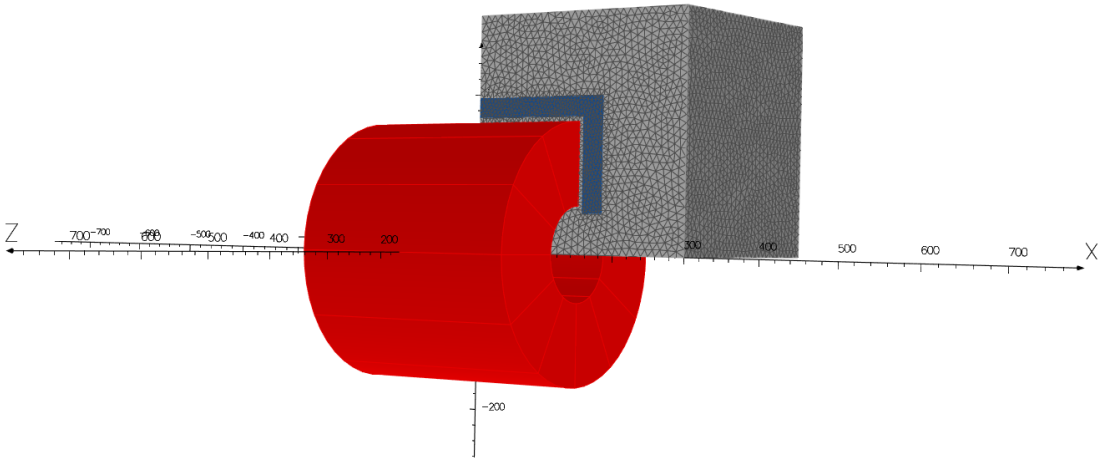

Fig. 13: Magnetic modelling of the solenoid magnet.

Table 9: Solenoid magnet coil parameters.

Solenoid magnet coil parameters	**Value**
Number of coils per magnet	21
Number of turns per coil	2x16=32
Number of cooling circuits	21
Conductor outer dimensions [mm]	6x6
Conductor cooling hole diameter [mm]	4.5
Conductor rounding edge radius [mm]	1
Conductor length per coil (approx.) [m]	22.7
Copper mass per coil (approx.) [kg]	3.9
Nominal resistance per coil at 20°C [mΩ]	20.1
Pressure drop [bar]	1
Cooling flow per coil [l/min]	0.76
Water spped [m/s]	0.8
Water temperature increase ^{o}C	20

The return yoke on both magnet ends shall be of a larger size, typically of 30 mm thickness for operation at 400 A, while originally designed with 20 mm thickness. Concerning the use of such magnet for the upgrade, a new magnet is required where the coils design of the present magnet (PXMLNAAIWP) can be used. The yoke shall be laminated with a 0.5 mm thick magnetic steel such as of grade M270-50A (see Table 9 and Fig.13). The dissipated power in the cooling circuit while the magnet is operated at 400 A in pulsed mode is 14.78 kW (considering an R.M.S. current of 185 A), which is suitable for the present cooling circuit performances.

The estimated costs of production of a full solenoid with one spare unit is approximately 60 kCHF. Design office costs are estimated at 15 kCHF. The need for a spare covers the risk assessment

evaluation in case of breakdown of the magnet with replacement within a short period of time. The supporting device with alignment can be recovered from the present setup. The lead time for the procurement, reception installation and commissioning is about 1.5 years.

The actual power converter is a S250 type that can deliver a maximum current of 250 A and will have to be replaced. Different solutions for powering have been investigated and the best option is to use a Polaris converter. Polaris is a new power converter family that has been developed for several consolidation programs (TT20 and North Area, AD, etc…). It is a modular converter where 'basic bricks' can be connected in different series/parallel configurations.

For this application a Polaris_2S converter is proposed to minimize the magnet current rise and fall times. The Polaris_2S is composed of two bricks with outputs connected in series. The Polaris_2S converter specifications are given in Table 10. This type of converter is not well adapted for fast pulses and, in this application, the output bandwidth is a limitation. The control loops may consequently have to be reviewed in order to increase their bandwidth.

Table 10: POLARIS_2S power converter parameters.

Polaris_2S converter parameters	**Units**	**Value**
Maximum peak operating current	[A]	400
Minimum operating current	[A]	0
Maximum output current (RMS)	[A_{RMS}]	250
Maximum average output power	[kW]	100
Current precision	[A]	40
Maximum output voltage	[V]	720
Magnet current rise time at I_{max}	[ms]	15
Magnet current rise time at I_{max}	[ms]	10
Maximum flat-top duration	[ms]	10
Repetition time	[ms]	100
Operation mode		p.p.m.
Remote control		FGC3 (Class 63)
Input voltage (3 phases)	[V_{RMS}]	400
Maximum input current (per phase)	[A_{RMS}]	200
Cooling		Water
Dimensions (width × depth × height)	[mm]	1800 × 900 × 2400
Weight	[kg]	1700

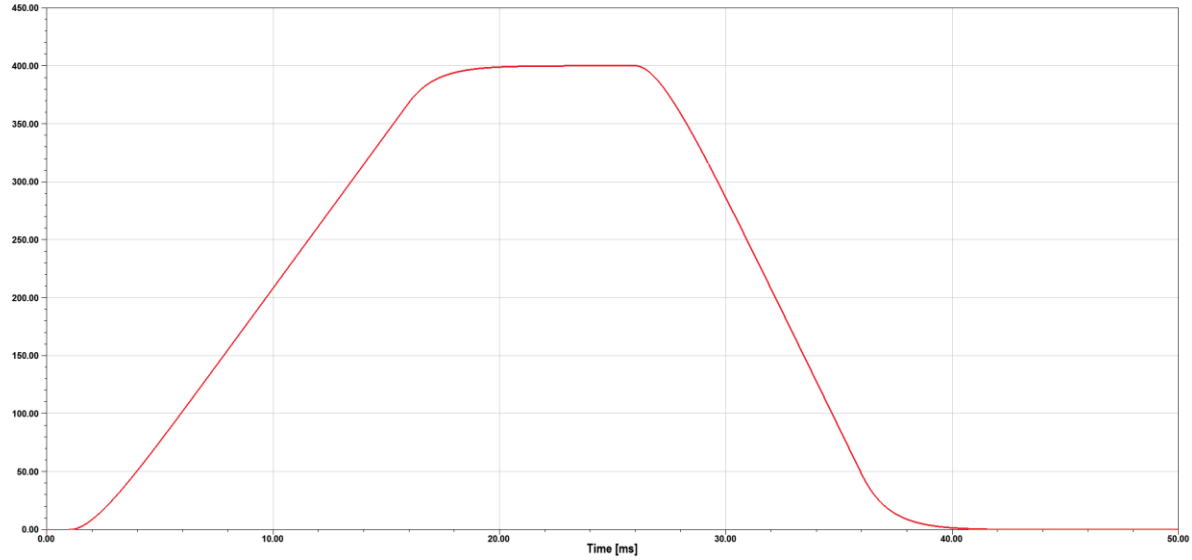

Figure 14: Magnet current with I_{ref} = 400 A and flat-top duration set to 10 ms

Considering the pulse shape given in Figure 14, the RMS output current is 185 A. The installation of the power converter has not been detailed but the cable length that has been taken into account corresponds to an installation in bldg. 351.

For the budget estimate, one spare converter is required. In this case, the cost for 2 converters is 210 kCHF where the cost of cabling (AC, DC, ethernet, interlocks, etc..) and installation (metallic support, false floors, etc…) are not included in the estimate. Regarding the schedule, the installation could take place during LS3 if a production is started in 2024.

6 Conclusions

This report summarizes the work carried out in the past couple for years towards designing a low-energy dedicated diagnostics line for Linac3 beam measurements near source extraction. Given the present absence of instrumentation devices in the sector, this line would give unprecedented opportunities to characterize in detail the beam parameters at this location and also provide insight in the physics of the source extraction mechanisms, that could help improve its stability and performance. The present performance of the source with Pb ions has taken nearly 20 years to achieve, and it has in part been so long due to the lack of instrumentation. In the event that operation with new types of ion species is approved for the future of the CERN ion complex, the beam diagnostics line would be an asset for optimization of the Linac3 source performance in as yet uncharted territories.

The report provides preliminary specifications for the magnets construction, and procurement of powering and instrumentation devices. An approximate costing for these components results in a price tag of about 270 kCHF for diagnostics and 490 kCHF for magnets and powering. No showstoppers have been identified for an installation target horizon in LS3, provided approval of the project is received by 2024. The cost of the quadrupoles and their powering is not included in this first estimate.

7 Acknowledgements

We would like to acknowledge the contribution to this study of Prof. C Valerio-Lizarraga from the University of Sinaloa and G R Montoya-Soto from the university of Guanajuato, Mexico, under the project Conacyt CF-2019/2042.

8 References

[1] OXY4LHC project kick-off meeting (2021).

[2] K.R. Crandall and D.P Rushtoi, “Trace3D documentation”, Los Alamos National Laboratory, New Mexico, USA, LA-UR-97-886 (1997).

[3] A. Perrin and J. Armand, “Travel V4.07 users’manual”, CERN, Geneva, Switzerland, internal note (2007).

[4] T. Kalvas, “IBSimu: a three-dimesional simulation software for charged particle optics”, *Review of Scientific Instruments*, vol. 81, 02B703 (2010).

[5] R. Alemany-Fernandez, talk at IEF workshop (2021).

[6] V. Toivanen *et al.*, Simulation of the CERN GTS-LHC ECR ion source extraction system with Lead and Argon ion beams, CERN-ACC-2014-0205 (2014).

[7] F. Roncarolo, document EDMS 2802860 (2022).

Appendix A **– Travel description of the diagnostics line.**

3 0.158 "Drift ";

19 0.234 3.32 "solenoid";

3 0.158 "Drift ";

3 0.3 "Drift ";

4 0.628 1.32 0 0 5. 1 39 0 1 39 0 2.8 0.45 "Bending magnet";

3 0.4 "Drift";

5 0.2 -6.7 100 0 0 0 0 "QUADRUPOLE";

3 0.2 "Drift";

6 1 3.2 3 100 0 0 0 "slit";

3 0.15 "Drift";

7 0 0 0 0 0 0 "Faraday Cup";

3 0.15 "Drift ";

5 0.2 2.25 100 0 0 0 0 "QUADRUPOLE";

3 0.5 "Drift";

3 0.5 "Drift";

7 0 0 0 0 0 0 "Faraday Cup";